Optimum back-pressure forging using servo die cushion

Optimum back-pressure forging using servo die cushion

Kiichiro Kawamoto[a,*], Takeshi Yoneyama[b], Masato Okada[b], Satoshi Kitayama[b], Junpei Chikahisa[b]

[a] *Product planning Dept.,Komatsu Industries Corp., 1-1 Ono-machi-shinmachi, Kanazawa-shi, Ishikawa 920-0225, Japan*
[b] *Institute of Science and Engineering,Kanazawa University, Kakuma-machi, Kanazawa-shi, Ishikawa 920-1192, Japan*

Abstract

This study focused on utilizing a servo die cushion (in conjunction with a servo press) as a "back-pressure load generator," to determine its effect on shape accuracy of the formed part and total forming load in forward extrusion during cold forging. The effect of back-pressure load application was confirmed in experiments, and the optimum setting pattern of back-pressure load was considered to minimize both shape accuracy of the formed part and back-pressure energy, which was representative of forming energy using a sequential approximate optimization. The precise back-pressure load control by the servo die cushion enabled the ideal load-pattern setting for optimization to be achieved.

Keywords: Forging; Forward extrusion; Back pressure; Servo die cushion

1. Introduction

Throughout its long history, forging has been generally used for mass production of automotive and electrical parts. Formed parts are generally not fully filled in the corner of the die, and secondary processing is required for the final figure. Various forming methods have been studied for net-shape forging in recent years. Back-pressure

---

* Corresponding author. Tel.: +81-762-293-4202; fax: +81-762-293-4348.
  E-mail address: kiichirou_kawamoto@komatsu.co.jp

application is a useful and powerful method to improve dimensional accuracy in complex parts, or to reduce maximum forming load in sheet forging. Osakada et al. (2000) improved shape accuracy of multiple extruded parts (fins) with a floating tool supported by pressure controls. Wang et al. (2010) indicated forming-load reduction for bottom compression drawing using a back-pressure load compared with backward extrusion. When using a back-pressure load, a special device is required in the die or die-set as the back-pressure load generator. Hydraulic power is mostly used for back-pressure control, and the response time and control accuracy using this method require improvement.

A servo die cushion, which is generally used in the servo press as a back-pressure generator for the drawing process, can be used as a back-pressure generator for the forging process. The merits of the servo die cushion—higher productivity and improved dimensional accuracy of the formed part—have been confirmed during sheet-metal drawing, compared with use of a hydraulic or pneumatic die cushion. Fewer application examples exist of the servo die cushion in forging than in sheet-metal drawing. The merits of the servo die cushion can be expected in forging because of its short response time and accurate pressure control.

On the other hand, the flexibility of the servo die cushion sometimes confuses the actual back-pressure setting for optimizing the objective function. In this study, by treating both the bottom unfilled area of the formed part as representative of shape accuracy and the back-pressure energy governing total forming energy as objective functions, the optimum back-pressure load-setting pattern was studied using the sequential approximate optimization in the model of simple forward extrusion.

2. Basic experiment

2.1. Objective and experimental model

The objective model was forward extrusion using an Al–Mg alloy of A5052 with phosphated treatment, as shown in Fig. 1. The die was installed in a 6300 kN AC servo press with a 400 kN servo die cushion used as a back-pressure load generator. The punch stroke was 7.8 mm and the outer punch stroke was 11 mm.
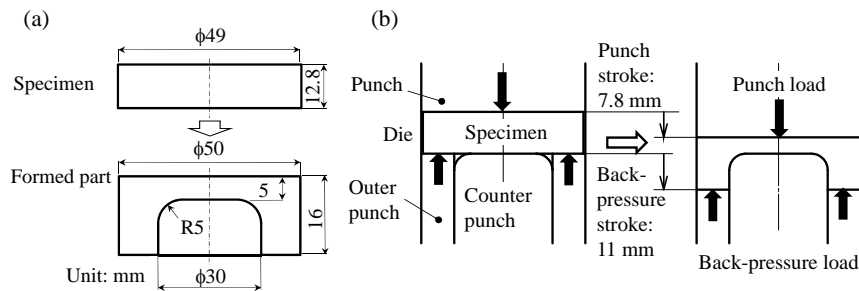

Fig. 1. Objective and experimental model: (a) Objective part; (b) Illustration of forming process.

2.2. Experimental method

The servo die cushion was programmed so that the back-pressure load was maintained at a set value. The experimental conditions of back-pressure load setting are shown in Table 1.

Table 1. Experimental conditions of back-pressure load setting.

Experiment No.	1	2-1	2-2	2-3	2-4	2-5	3
Punch stroke (mm)	7.8	7.8	7.8	7.8	7.8	7.8	7.3
Outer punch stroke (mm)	0	11	11	11	11	11	0
Back pressure load (kN)	0	50	100	110	125	150	-
Remark	Free forging	Back-pressure load application					Closed forging

The average punch speed was 4.0 mm/s in each experiment. The forming load was measured by strain gauges on the press frame. Dimensional accuracy of the formed part in each experiment number was measured by a three-dimensional measuring device. The unfilled area on the bottom part was evaluated as representative of the shape accuracy, as shown in Fig. 2. The maximum forming load and the unfilled area were evaluated as effects of back-pressure load application.
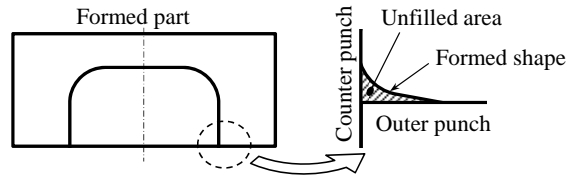

Fig. 2. Unfilled area.

2.3. Experimental results

The typical load and stroke diagrams are shown in Fig. 3. The maximum load was generated at around the end of forming at the 7.8 mm punch stroke, except in Experiment No. 3, where the punch stroke is restricted because of die strength.
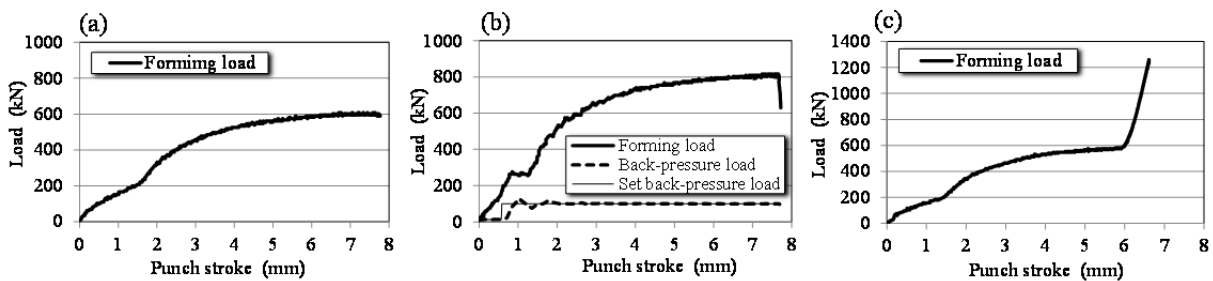

Fig. 3. Load and stroke diagrams: (a) Free forging/No.1; (b) Back-pressure forging/No.2-2; (c) Closed forging/No.3.

The relationship between maximum forming load and back-pressure load, and the relationship between unfilled area and back-pressure load are shown in Fig. 4.
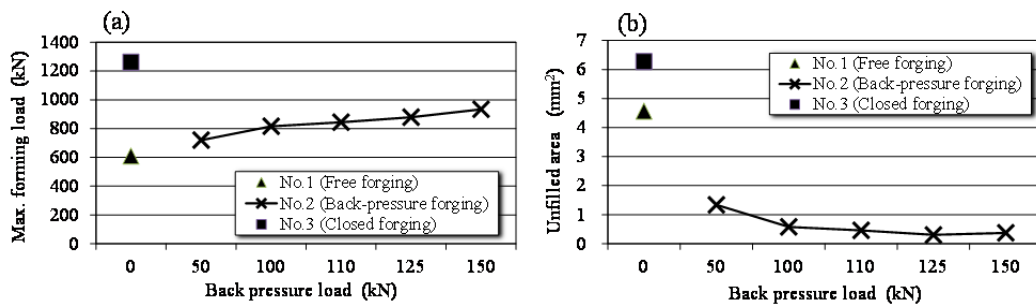

Fig. 4. Experimental results concerning back pressure load: (a) Relationship between maximum forming load and back-pressure load; (b) Relationship between unfilled area and back-pressure load.

The maximum forming load was proportionally increased in accordance with the back-pressure load increase. The unfilled area, however, decreased with back-pressure increase. In Experiment No. 3 (closed forging), the unfilled area was extremely high despite higher maximum forming load. Because the punch stroke was not enough

to form part thickness, material flow to the outer lower portion was short. Hence, back-pressure forging can reduce the unfilled area while simultaneously reducing the maximum forming load, compared with closed forging.

Fig. 5 shows the relationship between the maximum forming load and the unfilled area. This figure indicates that a trade-off relationship exists between the maximum forming load and the unfilled area. It is thought that an optimal back-pressure load setting may exist to minimize both the maximum forming load and the unfilled area.
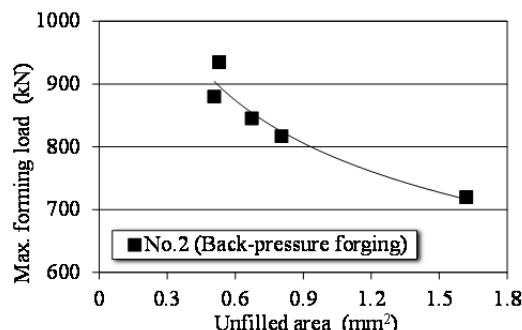

Fig. 5. Relationship between maximum forming load and unfilled area.

3. Optimization approach

3.1. Sequential approximate optimization

A sequential approximate optimization defined by Kitayama et al. (2011) is one of the optimization methods to finally obtain global optimized precise solutions to improve accuracy in response surface. According to the relationship shown in Fig. 5, the back-pressure load-setting pattern can be treated as a multiobjective optimization. The forming load is taken as the first objective function, and the unfilled area is also taken as the second. Back-pressure energy is replaced with the maximum forming load as the first objective function because back-pressure energy governs total forming energy, including the maximum forming load, where the back-pressure energy is the product of the back-pressure load and back-pressure stroke.

Computer-aided engineering was used, but the numerical simulation was time consuming. To save simulation time, the radial-basis function network, which was proposed by Kitayama et al. (2013), was adopted. The Pareto frontier was identified with a small number of simulation runs.

3.2. Optimization by simulation

The forging process was simulated using DEFORM-2D. The back-pressure load could be arbitrarily set along with the punch stroke. The setting pattern was divided into four portions to consider the response of the servo die cushion. The Pareto frontier, which was a set of optimal solutions obtained by simulation, and its optimal back-pressure load-setting pattern, are shown in Fig. 6. The back-pressure load-setting patterns with Roman numbers Ⅰ through Ⅲ in Fig. 6(b) correspond to the optimal solutions of the points with the same Roman numbers Ⅰ through Ⅲ in Fig. 6(a).

As shown in Fig. 6(a), a trade-off relationship exists between the back-pressure energy and the unfilled area. The characteristic experienced where higher back-pressure energy made the unfilled area smaller can be explained. It was found that the third step of the back-pressure load is effective to reduce the size of the unfilled area. The point of the third pressure load corresponds to a 3.9–5.9 mm punch stroke where the specimen passes the corner-R of the counter punch.
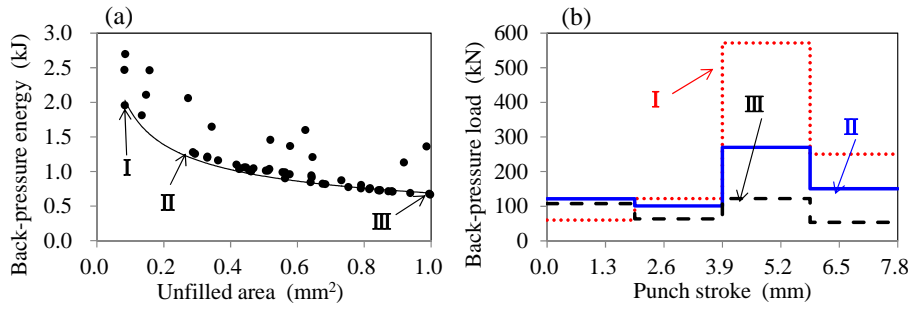
Fig. 6. (a) Pareto frontier; (b) Optimum back-pressure load-setting pattern.

3.3. Experimental confirmation of optimal setting pattern of back pressure load

The optimum back-pressure load-setting pattern was confirmed on the same servo press as the basic experiment. An example of the results is shown in Fig. 7, wherein the condition is the same as Ⅱ in Fig. 6. Fig. 7(a) shows the load and stroke diagram comparison between the simulation and the experiment. Fig. 7(b) shows the load and time diagram of the experiment. The experimental result of the back-pressure load followed the set value, though small over- and undershoots occurred at the changing point of each step load. The average punch speed was 2.6 mm/s in this condition. The error between the simulation result and the experimental result of the maximum forming load, the unfilled area, and the back-pressure energy are shown in Table 2. The numerical error of each evaluated item is small enough to simulate the actual forming performance using the optimal solution. Therefore, the optimization method proposed in this study is useful in the set conditions.
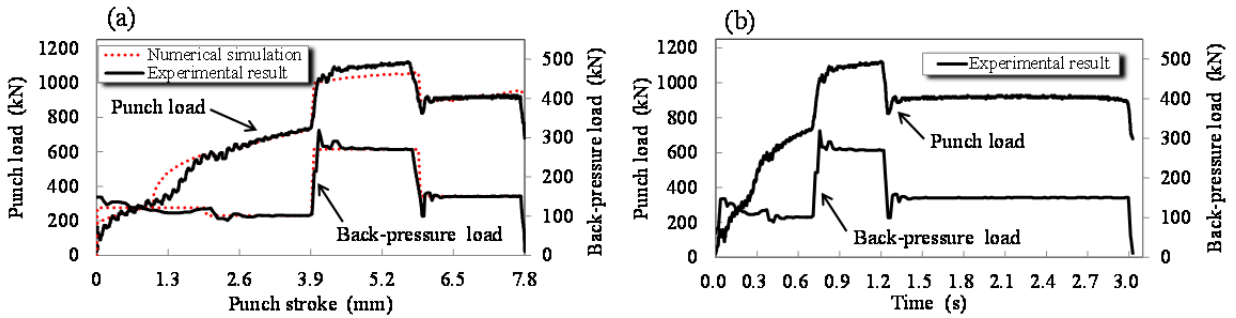

Fig. 7. (a) Load and stroke diagram using optimal back-pressure load setting; (b) Load diagram in time scale.

Table 2. Error between numerical simulation and experiment.

	Numerical simulation	Experimental result	Relative error %
Maximum forming load (kN)	1129	1061	6.41
Unfilled area (mm^2)	0.30	0.29	3.45
Back-pressure energy (kJ)	1258	1254	0.32

Cross sections of the formed parts were observed in both cases—the optimal back-pressure load application and free forging without the back-pressure load. The image and simulation of the cross section in the case of the optimal back-pressure load application whose pattern is same as the above condition is shown in Fig. 8. Another case of free forging without the back-pressure load is shown in Fig. 9. Comparing both cases, the back-pressure

load restricts material flow around part A in Fig. 8, and the material flow was accelerated to part B of the unfilled area. On the other hand, the material flow at B' in Fig. 9 tended to move outside because material flow was not restricted by the back-pressure load around A'. Hence, the back-pressure load application made the unfilled area smaller than with free forging, which does not restrict the material flow.
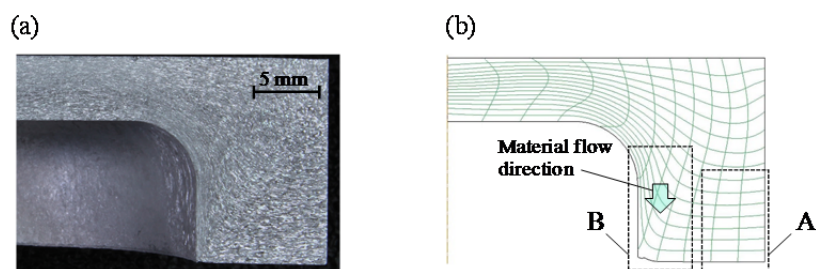

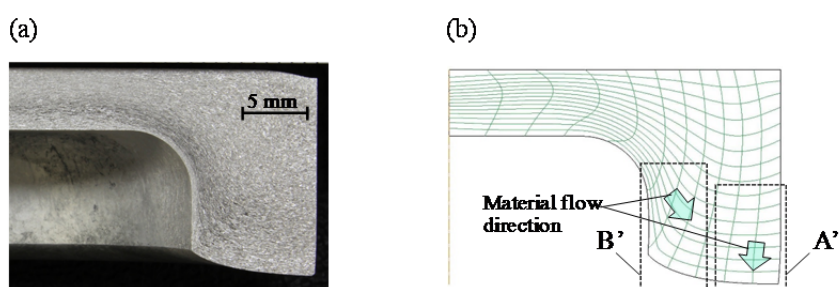Fig. 8. Cross-section in case of the optimal back-pressure load application; (a) Formed part; (b) Simulation.

Fig. 9. Cross-section in case of free forging without the back-pressure load application; (a) Formed part; (b) Simulation.

4. Conclusions

To improve the shape accuracy of a formed part and reduce the forming load during cold forging, the back-pressure load was applied by a servo die cushion to a simple forward extrusion model. The optimal back-pressure load-setting pattern was simulated as a multiobjective optimization problem to minimize the unfilled area and the back-pressure energy. The servo die cushion successfully followed the step-load variation in a short time and realized the simulation parameters for the optimal solution. The experimental results proved the effectiveness of the optimal solution using the servo die cushion.

References

Osakada, K., Hanami, S., Arai, N., 2000. Deformation Mode in Extrusion against Counter Pressure, Journal of the JSTP, 41(477), 1026–1030.
Wang, Z., Morishita, K., Ando, T., 2012. Boss Forming Technology by Bottom Compression Drawing, Journal of the JSTP, 53(616), 429–433.
Kitayama, S., Aakawa, M., Yamazaki, K., 2011. Sequential Approximate Optimization using Radial Basis Function network for engineering optimization, Optimization and Engineering, 12(4), 535–537.
Kitayama, S., Srirat, J., Arakawa, M., Yamazaki, K., 2013. Sequential Approximate Multi-objective Optimization using Radial Basis Function Network, Structural and Multidisciplinary Optimization, 48, 501–515.